Available online at www.sciencedirect.com
SCIENCE DIRECT®
Talanta 66 (2005) 1048–1062
Talanta
www.elsevier.com/locate/talanta

Microchip-based electrochromatography: designs and applications

Martin Pumera *

Department of Chemistry, Universitat Autonoma de Barcelona, E-08193 Bellaterra, Barcelona, Spain

Received 10 October 2004; received in revised form 20 December 2004; accepted 10 January 2005
Available online 3 February 2005

Abstract

Different techniques and methods of electrochromatography on "lab on a chip" devices are reviewed. Described approaches include open-channel microchip electrochromatography relying on C_8, C_{18} and novel gold nanoparticle (GNP) coating of microchannel wall; packed-channel microchip electrochromatography with new ways of automated loading and unloading of conventional octadecylsilica beads; monolith-based microchip electrochromatography with tailored casting of stationary phase at the specific places of microfluidic network and novel photolitographically fabricated collocated monolithic structures. Specific issues related to the microchip electrochromatography, i.e. importance of high aspect ratio of the microchannels in the open-channel electrochromatography or approaches eliminating the wall effect in the monolith-based electrochromatography, are discussed. Various applications for environmental, pharmacological, genomic and proteomic analysis are described. The operation parameters of reviewed microsystems are summarized in easy-to-read tables.
© 2005 Elsevier B.V. All rights reserved.

Keywords: Electrochromatography; Microchip; Miniaturization; Coating; Packing material; Monolith; DNA; Peptides; Review

1. Introduction

The development of micro total analytical systems, also called "lab on a chip", has witnessed explosive growth in the recent years [1–8]. Chip-based devices offer attractive features, such as the potential of fabrication of highly multiplexed systems with zero-dead volume interconnections, automation, mass-production; all this together with high throughput analysis, low solvent/reagent consumption and low cost. Particular attention has been given to the development of microchip zone electrophoresis (μCZE) [9–11]. Although microchip zone electrophoresis offers high separation efficiency (with theoretical plate height ∼1 μm [12]), due to short separation channels (in order of millimeters/centimeters), there is a major need for additional separation mechanism that would manipulate selectivity in the chip-based separation systems. Such selectivity manipulation can be achieved by microchip electrochromatography (μCEC).

Microchip-based electrochromatography is a hybrid method of microchip zone electrophoresis and chip-based liquid chromatography (μLC) and it combines the best characteristics of both methods. Separation mechanism of μCZE is based on the difference between mobilities of solutes, while in μLC it is based on the differences of partition coefficients between two phases. Combining μCZE with μLC creates a powerful analytical tool capable to separate both ionic and neutral compounds. Furthermore, plug-like electroosmotic

Abbreviations: 2D, two-dimensional; AA, acrylic acid; AIBN, azo-isobutyronitrile; AMPS, 2-acrylamido-2-methylpropanesulfonic acid; *β*, aspect ratio; BODIPY, 4,4-difluoro-1,3,5,7,8-pentamethyl-4-bora-3a,4a-diaza-(S)-indacene; COMOSS, collocate monolith support structures; μCEC, microchip-based electrochromatography; m-μCEC, monolithic microchip-based electrochromatography; o-μCEC, open-channel microchip-based electrochromatography; p-μCEC, packed-channel microchip-based electrochromatography; μCZE, microchip-based zone electrophoresis; EOF, electroosmotic flow; GNP, gold nanoparticle; *H*, theoretical plate height; μLC, microchip-based liquid chromatography; MES, 2-(*N*-morpholino)-ethanesulfonic acid; MPTMS, 3-methacryloxypropyltrimethoxysilane; MS, mass spectrometry; ODS, octadecylsilica; PAH, polycyclic aromatic hydrocarbon; PDADMAC, poly(diallyldimethylammonium chloride); PDMS, poly(dimethylsiloxane); PSG, photopolymerized sol–gel; PMMA, poly(methyl methacrylate); RP, reverse phase; SDS, sodium dodecyl sulfate; SSA, 4-styrenesulfonic acid; StMA, stearyl methacrylate; Tris, tris(hydroxymethyl)methylamine; VSA, vinylsulfonic acid

* Tel.: +34 93581 2118; fax: +34 93581 2379.
E-mail address: pumera@email.cz.

0039-9140/$ – see front matter © 2005 Elsevier B.V. All rights reserved.
doi:10.1016/j.talanta.2005.01.006

flow (EOF) profile results in reduced dispersion of the analyte zone, which increases column efficiency. Additionally, flow generated by electroosmosis obviates the use of high-pressure pumps, which are difficult to fabricate in the microchip manifold [13].

Since 1994, when the first μCEC work was published by Ramsey and co-workers [14], the microchip electrochromatography has received considerable attention. The aim of this review is to cover the time span of the last 11 years (1994–2004) while focusing on the main modes of μCEC; (i) open-channel electrochromatography (o-μCEC) in which the walls of microchannel are coated with stationary phase; (ii) packed-channel electrochromatography (p-μCEC) in which microchannels are filled with typical RP-HPLC packing materials; (iii) continuous rod electrochromatography in which channels contain monolithic stationary phase prepared by in situ polymerization or monoliths directly microfabricated using lithographic methods (m-μCEC).

2. Microchip electrochromatography: designs and applications

2.1. Open-channel electrochromatography (o-μCEC)

In o-μCEC the walls of a microchip channel are coated with the selector. Different distribution equilibrias between the running buffer and coated stationary phase are responsible for tailoring the selectivity and improved resolution of the solutes. As the diameter of the open channel decreases, the resistance to mass transfer decreases too [15] but other problems arise. For example, the smaller the surface of the modified channel is the more problems with the separation channel overloading are. Also injection and detection volumes must be scaled down proportionally to prevent excessive contributions to band broadening and therefore may fall bellow the limit of detection. To minimize these problems, channels with high aspect ratio (β) of the channel width to the channel height are fabricated (for an example, see Fig. 1). This allows improved mass transfer in one dimension while the sample load and detection volume is maintained in the other dimension [14]. The channel dimensions and the aspect ratios of reviewed o-μCEC articles are summarized in Table 1.

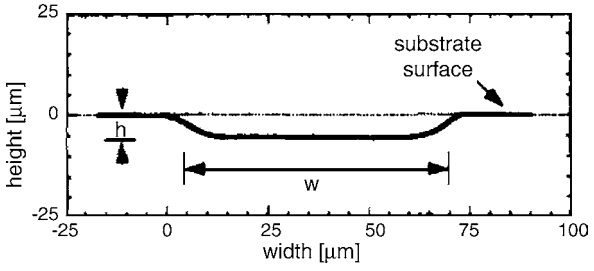

Fig. 1. Typical profile of channel cross section in open-channel microchip electrochromatography. High aspect ratio ($\beta = w_{1/2}/h$; where $w_{1/2}$ is the channel width at half-height, h is the channel height) improves mass transfer in one dimension while the detection is carried out in the other dimension. Reprinted from ref. [14] with permission.

2.1.1. C_{18} and C_8 reverse phase

The octadecyl reverse-phase coating is popular in microchip-based o-μCEC. The chemistry of the octadecyl (C_{18}) group bonding on a glass surface is well documented [16]. The first instance of microchip o-μCEC was described by Ramsey and co-workers [14]. They prepared glass microchip with serpentine column geometry and chemically-bonded octadecyl group (using chlorodimethyloctadecylsilane as a precursor) on the microchannel walls. To maintain high efficiency without sacrificing the detection path length or injection/detection volumes, the rectangular channel geometry with high aspect ratio $\beta = 12$ was used. Three neutral coumarin dyes were baseline separated in 170 s using effective separation channel length of 58 mm. For coumarin 440, plate height (H) 5 μm was observed, while the most retained component, coumarin 460, had $H = 45$ μm.

Another method for development of RP o-μCEC based on glass chip substrate was developed by Constantin et al. via sol–gel technique [17]. They produced stationary phase which contained silanol groups generating EOF and C_8 groups mediating the separation using tetraethoxysilane (TEOS) and octyltriethoxysilane as co-monomers. Separation of three polycyclic aromatic hydrocarbons was performed in 6.5 min. They compared the performance of chip-based o-μCEC with conventional capillary o-CEC coated by the same technique. Performance of the microchip μCEC was found to be slightly better in comparison to the conventional o-CEC [17].

Besides the glass-based devices with high aspect ratio channels, which are usually fabricated by chemical wet etching [14], the polymer-based substrates also offer possibility for manufacturing high-aspect ratio microstructures [18]. However, due to different technology of microfabrication of polymer chips the high aspect ratio is usually obtained by designing narrow and deep channels [19,20], contrary to glass-based isotropic etching technology, which allows to produce shallow and wide microchannels [14]. Polymeric poly(methyl methacrylate) (PMMA) microchip device for C_{18} reverse phase o-μCEC separation of DNA fragments was prepared by Soper and co-workers [19–22]. To modify the PMMA channel with C_{18} moiety, the bare PMMA surface was aminated with 1,2-diaminoethane or 1,3-diaminopropane. The following reaction with *n*-octadecane-1-isocyanate resulted to well-organized and highly crystalline C_{18} surface. While the unmodified PMMA is generally dissoluble by mobile phase containing acetonitrile, now the uniform C_{18} layer protected the underlying PMMA well. The C_{18}-modified PMMA was stable even upon long-term exposure to acetonitrile-based mobile phase. The EOF in C_{18}-modified channel was anodic because of unreacted amine groups. These resulted in an excess surface charge that was positive, producing the EOF reversed—compared to native

Table 1
Open-channel microchip electrochromatography (o-μCEC)

Stationary phase/chip material	Mobile phase	Channel dimensions (width[a] × depth)	β[b]	Analyte	Time of analysis (s)	Efficiency (H) (μm)	Reference
C_{18}/glass	Sodium tetraborate (10 mM, pH 9.2) with 25% (v/v) acetonitrile	66 μm × 5.6 μm	12	Coumarin dyes (C440, C450, C460)	170	5	[14]
C_{18}/glass	Sodium tetraborate (10 mM, pH 8.4) with 15–50% (v/v) acetonitrile	23–56 μm × 2.9–10.2 μm	5–10	Coumarin dyes (C440, C450, C460, C480)	20	2	[27]
C_{18}/glass	Sodium tetraborate (10 mM) with 30% (v/v) acetonitrile and 0.1% (v/v) trifluoroacetic acid	34–212 μm × 10.8 μm	3–20	Products from tryptic digests of β-casein	780	1.4	[29]
C_{18}/glass	Tris (10 mM, pH 8.2) with 20–56% (v/v) acetonitrile	22 μm × 5 μm	4	PAHs (anthracene, pyrene, 1,2-benzofluorene, benzo[*a*]pyrene)	50	0.9	[28]
C_8/glass	NaCl (10 mM) with 50% (v/v) acetonitrile	90 μm × 23 μm	4	PAHs (naphtalene, pyrene, phenantrene)	390	N/A[c]	[17]
C_{18}/PMMA	Triethylammonium acetate (50 mM, pH 7.4) with 25% (v/v) acetonitrile	100 μm × 100 μm	1	DNA fragments (100, 200, 400, 800, 1200, 2000 bp)	140	N/A	[22]
C_{18}/PMMA	Triethylammonium acetate (50 mM, pH 7.4) with 25% (v/v) acetonitrile	15 μm × 85 μm	6	DNA fragments (100, 200, 400, 800, 1200, 2000 bp)	140	24	[19]
C_{18}/PMMA	Triethylammonium acetate (30 mM, pH 7.4) with 0–30% (v/v) acetonitrile	15 μm × 85 μm	6	DNA fragments (PCR products and sizing ladder 100, 200, 400, 800, 1200, 2000 bp)	80	∼37	[20]
Gold nanoparticles/glass	Sodium acetate (20 mM, pH 5.0)	50 μm × 20 μm	2.5	Aminophenols (ortho, meta, para)	160	26	[32]
Gold nanoparticles/PMMA	Glycine-citrate (100 mM, pH 9.2)	75 μm × 75 μm	1	ds-DNA markers (8–2176 bp)	480	N/A	[33]
Phenyl; C_{11} alcohol/polyester	Sodium tetraborate (50 mM, pH 9.6)	100 μm × 15 μm	7	Sulforhodamine B and sulforhodamine 101	810	13	[36]
Phenyl; C_4, C_7, C_{11} alcohols/polyester	Sodium tetraborate (25 mM, pH 9.6)	72 μm × 8 μm	9	Sulforhodamine B and sulforhodamine 101	600	7	[37]

[a] Channel width at half-height ($w_{1/2}$).
[b] Aspect ratio, $\beta = w_{1/2}/h$.
[c] N/A: information is not available.

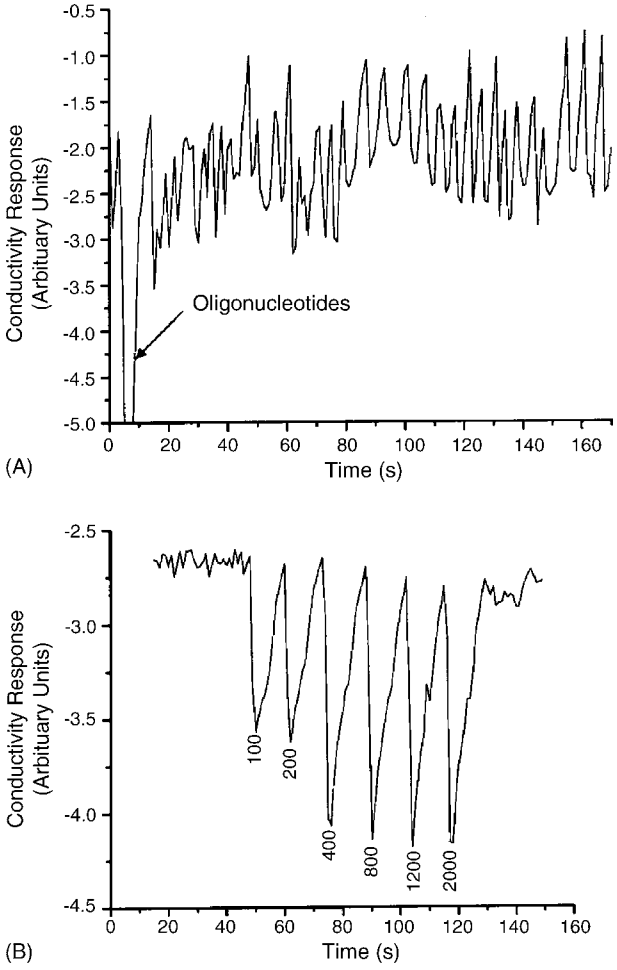

Fig. 2. Open-channel μCEC separation of a double-stranded DNA ladder in an unmodified (A) and C_{18}-modified (B) PMMA device. The ladder consisted of 100, 200, 400, 800, 1200 and 2000 bp fragments. The PMMA microchannel was modified by chemically attaching a C_{18} phase to its surface. The mobile phase used for this separation was 25% acetonitrile and 75% aqueous phase containing 50 mM TEAA (ion-pairing agent, pH 7.4). Detection was accomplished using indirect, contact conductivity detection. The field strength used for the separation was 100 V/cm. Reprinted from ref. [19] with permission.

PMMA. Six DNA fragments were well separated using C_{18}-PMMA chip-based device while an unmodified PMMA chip showed poor performance (see Fig. 2) [19,22]. Influence of various solvent (acetonitrile/water) strength on the EOF, separation efficiency and the time of analysis was also studied [20]. The electroosmotic mobility was found to rise with increases in organic modifier content in background electrolyte. Retention factor of ion-paired DNA complexes decreased as the acetonitrile content increased. The selectivity showed maximum at 20% acetonitrile in mobile phase, while the plate numbers and resolution decreased as the acetonitrile concentration increased. These results were similar to what was observed in conventional C_{18}-CEC fused silica capillaries [23,24].

The ability to design and fabricate chip manifolds with low-volume connections offers great possibilities for precise

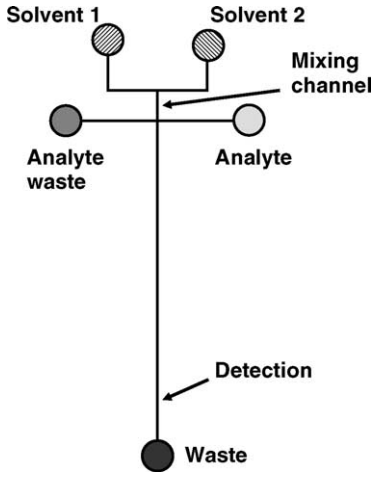

Fig. 3. Schematic design of the on-chip mixing scheme. Solvent-programmable microfluidic device consists of a channel cross which is used for injection and a mixing channel at one of the side arms, where the two different solvents are mixed. The ratio of mixing can be either held constant over a run (isocratic conditions) or can be varied with time (gradient conditions). Based on refs. [25,27] with permission.

on-chip mixing of mobile phase and therefore opens many ways for high efficient gradient elution (Fig. 3). This is extremely beneficial for complex mixtures' separations, where isocratic elution is not suitable. On-chip mixing is a great advantage of microchip-based systems compare to the conventional CE/CEC, where the gradient elution is a very complicated issue [26]. Kutter et al. extensively studied solvent programming on C_{18}-modified glass-chip platform [27]. The parameters influencing electrochromatographic separation, such as channel depth (2.8–10.2 μm), different coating efficiencies (using silanizing agents octadecyltrimethoxysilane or octadecyldiisobutyl(dimethylamino)silane), mixing ratio and composition of mobile phase, were investigated. It was found that with the decrease of the channel depth, the plate height decreases too, following theoretical predictions. However, the differences in plate numbers between channel depths of 4.7 and 2.9 μm were very small. Since manufacturing and operating chips with channel depth <3 μm is challenging, the optimal channels used in this work were 5.2 μm deep (corresponding plate height of such channel was ∼2 μm). Fluid control in the microchips during injection and during isocratic or solvent-programmed analysis was accomplished by applying voltages to the reservoirs in an appropriate fashion. The voltage for the two mobile phase reservoirs leading into the mixing channel varied over time for gradient experiments. Linear gradients with different slopes, initiation times, duration times, and start percentages of organic modifier were examined to tailor selectivity and analysis time of the separation of four neutral coumarin dyes (C440, C450, C460, C480). Even very steep gradients (acetonitrile from 29 to 50% within 5 s) produced very good efficiencies, with analysis times of a 20 s for a four-component mixture of coumarin dyes.

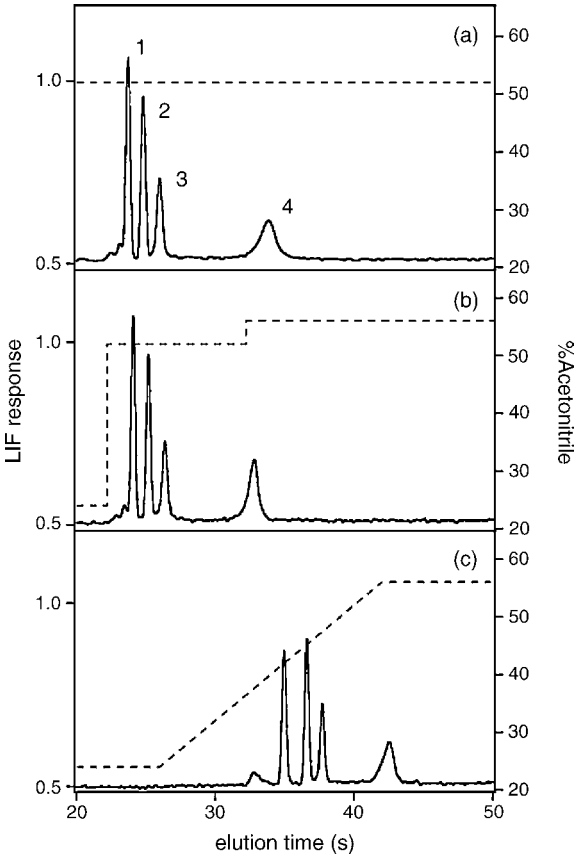

Fig. 4. Solvent-programmed open-channel microchip electrochromatography. (a) Isocratic, (b) step gradient and (c) linear gradient separations of (1) anthracene, (2) pyrene, (3) 1,2-benzofluorene and (4) benzo[*a*]pyrene. The concentrations of analytes 1–4 were 2.8, 0.9, 5.8 and 5.0 μM, respectively. The dashed lines show the gradient profiles. Reprinted from ref. [28] with permission.

The coating with octadecylsilane groups lead to a decrease of the EOF only by 10–25% when compared to an untreated channel of a glass chip. There was found no apparent correlation between different depth of the channels or the aspect ratios and the corresponding EOF reduction. To expand the application scope of the solvent programmed platform, the same group developed μ-TAS device integrating solvent programmed C_{18} RP separation of four PAHs (shown in Fig. 4) with preconcentration and the sample filtration steps [28].

The advantage of the manipulation of the sample with minimal or zero dead volumes between interconnecting channels of microchip-based systems was further exploited by Gottschlich et al. in their work on 2D microchip electrochromatography/zone electrophoresis [29]. The planar glass microchip device consisted from a 250 mm separation channel with spiral geometry for o-μCEC connected to a 12 mm straight separation channel for μCZE, as shown in Fig. 5. This new concept was demonstrated on 2D separation of β-casein tryptic digest products. The first dimension of the separation (o-μCEC based on C_{18} RP) was operated under isocratic conditions and the eluent from o-μCEC was repetitively injected to the second dimension every few seconds. Ideally, the separation mechanisms of the 2D separation methods should be orthogonal. In such a case, the peak capacity of 2D method is equal to peak capacity of the first separation method multiplied by peak capacity of the second separation method. Since o-μCEC as the first dimension was the hybrid method of reverse-phase liquid chromatography and microchip zone electrophoresis, and second dimension relied on free solution microchip zone electrophoresis, it is clear that these methods were not fully orthogonal. Due to correlation in o-μCEC and μCZE separation mechanisms, not all 2D area was accessible. However, 50% increase of the information content was achieved when going from 1D o-μCEC to 2D o-μCEC/μCZE system. Similar 2D microfluidic devices for peptide/proteomic analysis were published by the same group [30,31]. These were based on 2D combination of microchip micellar electrokinetic chromatography (MEKC) and μCZE.

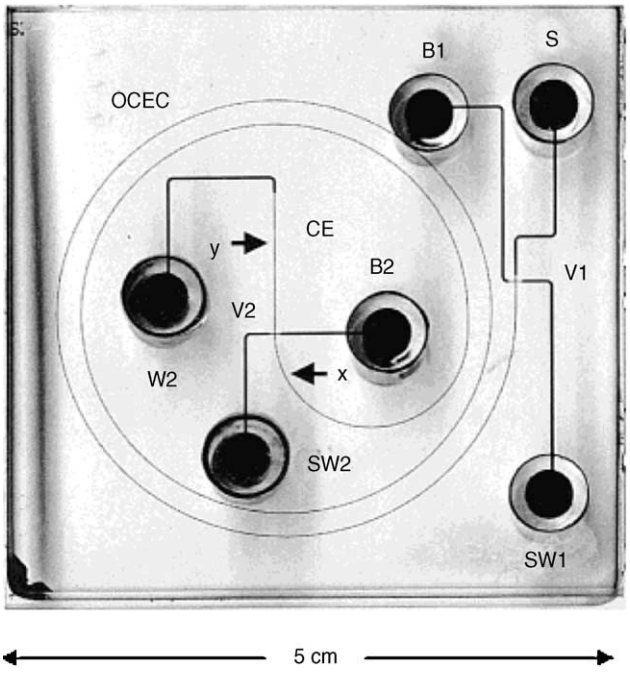

Fig. 5. The microchip used for 2D separations. The separation channel for the first dimension (o-μCEC) extends from the first valve V1 to the second valve V2. The second dimension (μCZE) extends from the second valve V2 to the detection point y. Sample (S), buffers 1 and 2 (B1, B2), sample waste 1 and 2 (SW1, SW2), and waste (W) reservoirs are positioned at the terminals of each channel. The arrows indicate the detection points in the o-μCEC channel (x) and μCZE channel (y). The channels and reservoirs are filled with black ink for contrast. Reprinted from ref. [29] with permission.

2.1.2. Gold nanoparticles

Pumera et al. described first the use of gold nanoparticles (GNPs) in conjunction with microchip-based electrophoresis to improve the selectivities between solutes and to increase the efficiency of the separation [32]. They coated the glass wall of a channel of a microfluidic device with a layer of poly(diallyldimethylammonium chloride) (PDADMAC) and 10-nm citrate-stabilized gold nanoparticles were collected on such modified channel. The resolutions and the plate numbers

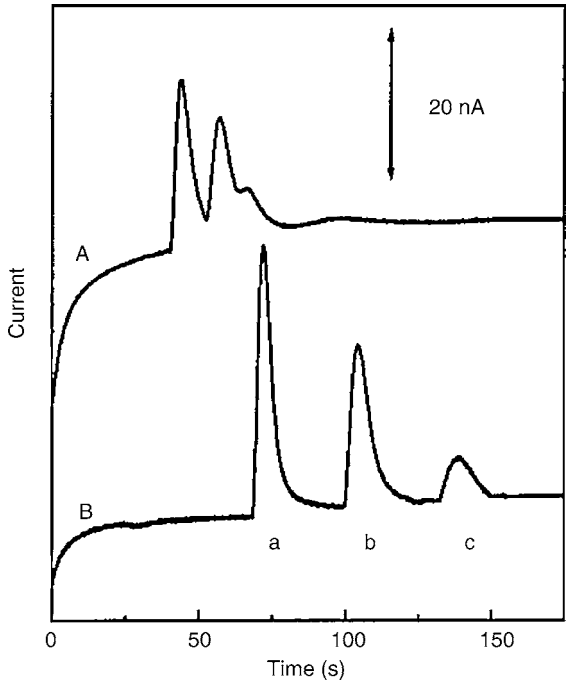

Fig. 6. Gold nanoparticle enhanced open-channel microchip electrochromatography. Electrophoregrams showing the separations of 1 mM *p*-aminophenol (a), *o*-aminophenol (b) and *m*-aminophenol (c) in a bare glass channel (A) without treatment and (B) after PDADMAC-gold coating. *Conditions:* acetate buffer (20 mM, pH 5.0) as an electrophoresis buffer; sample injection at +1500 V for 3 s; separation voltage, +2000 V; detection at +0.8 V using a gold-coated screen-printed carbon electrode. Reprinted from ref. [32] with permission.

of studied aminophenols were doubled in the presence of the gold nanoparticles when compared to untreated channel, as shown in Fig. 6. Such selectivity improvements reflected changes in the observed mobility accrued from interactions of solutes with the nanoparticle surface. It is assumed that retention mechanism of solutes on gold nanoparticles (which are protected by monolayer of organic molecules, i.e. citrate or alkylthiols) originate from both solute–organic monolayer and solute–gold nanoparticle surface interactions [32–35].

The application range of GNPs was later extended for larger biomolecules by Lin et al. [33]. The separation channel of a poly(methyl methacrylate) (PMMA) microchip was coated subsequently with poly(vinyl pyrrolidone) and poly(ethylene oxide), respectively. Afterwards, 13-nm citrate stabilized gold nanoparticles were collected on it. The GNPs coated PMMA device showed improved reproducibility and resolution of double stranded DNA markers (size ranging from 8 to 2176 bp). Both groups [32,33] found that the GNPs coated chips were stable for more than 1 month and that the day-to-day reproducibility of the migration times was good (R.S.D. < 3%).

The EOF in untreated glass channels depends heavily upon the negative charges of the silanol groups of the internal wall surface. The coating of the wall with gold nanoparticles resulted in a decrease of the EOF about 40%, in comparison to an untreated channels, because free silanol groups on the channel surface were masked, due to adsorption of GNPs on glass microchannel wall [32]. Similar effect of ∼40% decrease of EOF showed PMMA channel coated with GNPs [33].

2.1.3. Bulk microchip material modifications

Xu et al. developed an alternative approach to o-μCEC wall modification. In contrary to the surface modifications of glass or polymer-based devices, which were described in the Sections 2.1.1 and 2.1.2, the authors incorporated the appropriate selector molecules into the whole bulk material of microchip by copolymerization [36,37]. The polyester chip modified with 10-undecen-1-ol showed dramatically improved separation efficiency and resolution when compared to the fused silica capillary [36]. The same group further studied influence of different moieties (4-pentene-1-ol, 7-octene-1-ol and 10-undecene-1-ol) added to the prepolymers on the separation efficiency [37]. They concluded that with decreasing length of build-in alcohols the separation efficiency increases. Varying the length of alkylalcohol chain allows tailoring the selectivity. However, it is important to critically note that the best resolution of two dyes was achieved in polyester chip without any modification. A major and distinct advantage of this new method is that the surface chemistries can be modified during the fabrication process itself. Further exploration of bulk polymeric modifications in other materials (i.e. PMMA) is currently in the process [38].

2.2. Packed-channel electrochromatography (p-μCEC)

Further lowering mass transfer resistance in open-channel electrochromatography needs to reduce dimensions of its channels. However, there are considerable difficulties with using open channels with widths 3 μm or less, such as difficult manufacturing, clogging and low detection volume [27]. Contrary, packed beds have the benefit of providing of low mobile phase mass transfer resistance and wide variety of stationary phases available. Furthermore, p-μCEC can utilize commercially prepared, reproducible stationary phase materials developed for HPLC. Stationary phase is usually held in the position by frits or weirs. Type of stationary phase, frite type, bed dimensions and efficiency of reviewed p-μCEC articles are summarized in Table 2.

Electroosmotically driven microsystem with two weirs integrated in a glass substrate was constructed by Harrison and co-workers [39,40]. One micrometer high weirs enclosed 330-pL cavity in which 1.5–4.0 μm octadecyl coated silica beads were placed. The beads were loaded and removed from the separation chamber using electroosmotic flow through special introducing channel (as shown in Fig. 7). The different loading channel and cavity geometries were tested. Several two-composite mixtures were successfully separated on 200 μm long C_{18} column, such as fluorescein and BODIPY within 20 s [39], BODIPY and acridine orange in 10 s and angiotensin II-alexafluor from excess of labeling agent, alexafluor, in 18 s [40]. To expand peak capacity of such p-μCEC

Table 2
Packed-channel microchip electrochromatography (p-μCEC)

Stationary phase/chip material	Stationary phase size (μm)	Frit type	Mobile phase	Bed dimensions (width[a] × depth × length)	Analyte	Time of analysis (s)	Efficiency (H) (μm)	Reference
C_{18}/glass	1.5–4	Two 1 μm high build-in weirs	Ammonium acetate (50 mM, pH 8.5) with 30% (v/v) acetonitrile	580 μm × 10 μm × 200 μm	BODIPY and fluorescein	20	10–20	[39]
C_{18}/glass	1.5–4	Two 1 μm high build-in weirs	Ammonium acetate (5 mM, pH 8.3) with 40% (v/v) acetonitrile (for BODIPY and acidine orange); 0.05% trifluoroacetic acid and 26% acetonitrile in water for angiotensin II-alexafluor and alexafluor	580 μm × 10 μm × 200 μm	BODIPY and acridine orange; angiotensin II-alexafluor and alexafluor	18	2.4	[40]
C_{18}/glass	1.5–4	Two 1 μm high build-in weirs	Tris (25 mM, pH 8.0) with 80% acetonitrile for fluorescent dyes; 10 mM MES buffer, pH 6.7, with 50% (v/v) acetonitrile for analysis of aminoacids	100 μm × 10 μm × 1–5 mm	BODIPY, acridine orange and rhodamine; arginine and leucine	20	2.8	[41]
C_{18}/PDMS-glass	3	Taped by keystone effect	Phosphate (5 mM, pH 7.0) with 20% (v/v) acetonitrile	70 μm × 30 μm × 15 mm	Benzaldehyde and methanol	10	3.5	[42]
C_4/PDMS-quartz	5	Stabilized by sol–gel	MES (20 mM, pH 6) with 5% (v/v) acetonitrile	250 μm × 43 μm × 25 mm	Dipeptides Trp-Ala, Leu-Trp, Trp-Trp	500	N/A	[44]
C_{18}/PDMS	5	Integral hexagonal structures of micrometer size	Tris (5 mM) and borate buffer (20 mM), pH 9.0 with 50% (v/v) acetonitrile	150 μm × 25 μm × 3 mm	Coumarin 440 and 450	90	N/A	[45]

[a] Channel width at half-height ($w_{1/2}$).

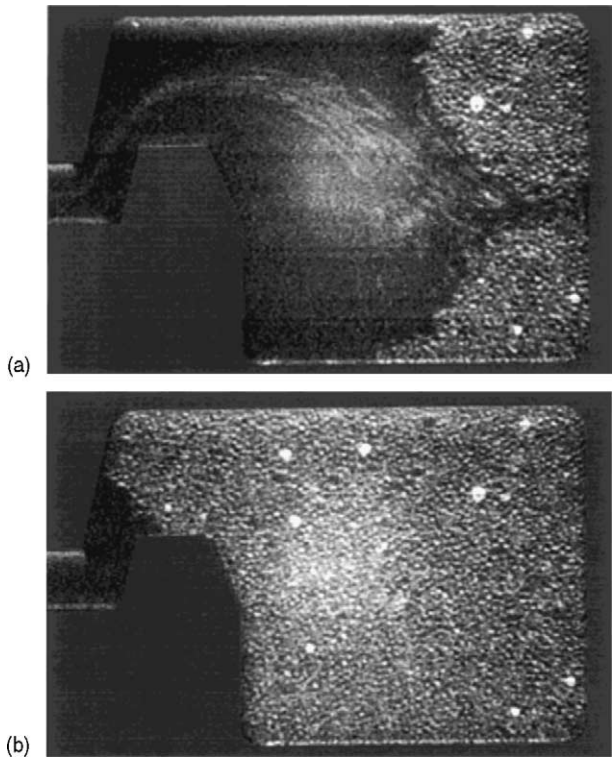

Fig. 7. Packed-channel microchip electrochromatography with electrokinetically loaded and removed beads. Images of the chamber (a) at an initial stage of electrokinetic packing and (b) after it is completely filled with beads. Image background has been colored to enhance contrast. Reprinted from ref. [39] with permission.

column, it was necessary to increase the length of packed bed. The same group constructed similar two-weir design with longer (1–5 mm) μCEC columns [41]. Electrokinetic packing of the columns 1 mm or longer proved to be difficult compared to 200 μm columns and it needed to be combined with pressure packing. Furthermore, the beads had to be permanently trapped in the bed to ensure stability of packed column by polymerization of a methacrylate monomer within the bead introduction channel. One and two millimeter long columns were found to be stable for μCEC separation after blocking the bead introduction channel, 5 mm columns showed voids even after this procedure. BODIPY, acridine orange and rhodamine were baseline separated within 20 s and arginine and leucine within 10 s, both experiments using 1 mm long column.

Ro et al. constructed PDMS microchip with build-in integrated hexagonal structures which served as inlet and outlet frits [45]. Size of each of the PDMS hexagons was 25 μm × 20 μm and spacing between them 3 μm, allowing to entrap 5 μm C_{18} beads. Microparticles were introduced by special side loading channel using pressure applied by syringe. Common disadvantage of PDMS material, such as unstable EOF and adsorption of some unpolar species was overcome by dynamic coating, using polybrene and dextran sulfate. Two coumarin dyes were separated in 90 s by 3 mm long and 150 μm wide column.

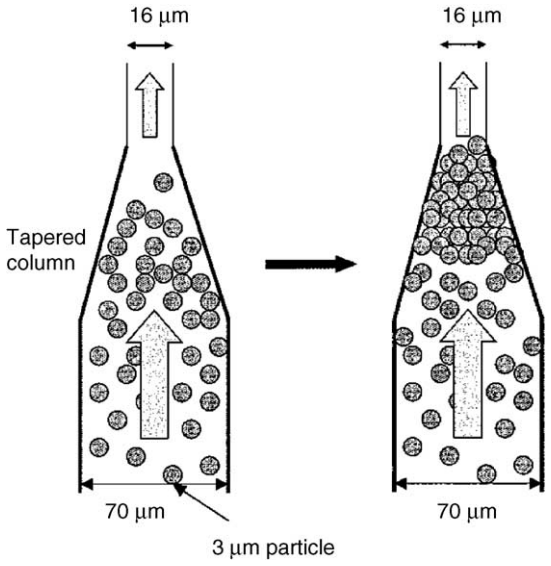

Fig. 8. Diagram of the microchannel-based "keystone effect". A suspension of ODS modified particles is drawn from the waste reservoir toward the taper by vacuum. At the taper, the density of the particles increases, and they aggregate without requiring a physical barrier or frit. These first particles act as the "keystones", blocking the others and allowing the packed segment to grow longer in the opposite direction. Reprinted from ref. [42] with permission.

Original approach to realize fritless p-μCEC device presented Ceriotti et al. [42]. Particles with diameter 3 μm were spatially retained and packed without the need for frit structures of any kind using "keystone effect" [43] in the tapered geometry at the beginning of PDMS channel, as shown in Fig. 8. Microspheres covered with C_{18} groups were loaded using vacuum and stopped at the taper, but the simple use of a vacuum was not sufficient to make them stable for μCEC separation. Stabilization of the packing was achieved by placing the chip in the oven overnight at 115 °C. Such operation resulted in the interparticle bonding and stable ODS bed. Several parameters influenced the "keystone effect" at the taper. As it can be expected, the concentration of particles in the suspension was found to be critical. At higher concentrations, the particles tended to aggregate somewhere in the separation column before reaching the taper, but at lower concentrations, the particle density at the taper was insufficient and did not provide "keystone effect". On the other hand, different length of taper did not have any significant influence upon packing process when tapers of 0.5, 0.8 and 1.0 mm length were examined. A mixture of benzaldehyde and methanol was separated within 10 s using 15 mm long column.

Jindal and Cramer developed another fritless approach allowing localized immobilization of packed bed in desired part of the separation channel [44]. Microfluidic network was etched in the quartz while leaving the channels unenclosed by cover plate. Only a selected part of the separation channel was reversibly sealed with PDMS plate creating a temporary channel. Sol–gel containing 5 μm C_4 particles was

easily loaded in such temporal channel by a vacuum pump. Once the sol–gel stabilized the stationary phase, the temporal reversible PDMS plate was removed and the whole microfluidic network was irreversibly sealed by another PDMS substrate. A mixture of three dipeptides was separated in 7 min. Despite the original approach of packed bed stabilization, the microsystem showed poor efficiency and further optimization of the stationary phase is needed.

2.3. Microchip electrochromatography with monolithic stationary phases (m-μCEC)

Achieving the uniform packing of microchannels with beads can be a very challenging task in p-μCEC [41]. Problems in channel packing can lead in irregularities in packed bed and in a poor efficiency of the system. Peak broadening can be caused by the inlet frit. Moreover, frits contribute to formation of the bubbles. These problems can be overcome by preparing a microchannel consisting of a block of a porous solid, called monolith or rod, manufactured by in situ polymerization or by microfabrication technique.

2.3.1. Monoliths prepared by in situ polymerization

The preparation of the continuous bed is relatively easy, since a monomer solution with low viscosity is simply pressed into the channels. This way high efficient columns can be fabricated without limitations of p-μCEC. Monomer mixture composition allows an easy manipulation of separation parameters, such as hydrophobicity, pore size and charge. Monolithic separation phases for microchip CEC can be manufactured in two different ways: by a chemical initiation which results in a microchip with channel continuously filled with polymer or by photopolymerization which allows to create polymer bed at the specific places of the microfluidic network.

2.3.1.1. Chemical initiation. Separation microsystem based on continuous rod of covalently linked 0.1–0.4 μm polymer microstructures was prepared by chemically initiated copolymerization of piperazine diacrylamide, methacrylamide, *N*-isopropylacrylamide and vinyl sulfonic acid [46]. Such reaction (performed overnight) resulted in monolithic column providing SO_3^- groups for the generation of electroosmotic flow in wide spectrum of pH and isopropyl groups (C_3) for weak reversed-phase separation. The rod was covalently attached to the channel walls to eliminate "wall effects" [47]. Six alkylphenones and three tricyclic antidepressants were successfully separated in 18 min. To speed up the separation, shorter monolithic columns with a higher sulfonic acid group density to generate faster EOF was prepared and uracil, phenol and benzyl alcohol were separated in 20 s. The comparison of efficiencies of the microchip and capillary CEC with the same cross-section area was performed. The results showed no significant difference between plate heights of chip and conventional CEC systems.

2.3.1.2. Photoinitiation. Since polymerization of monolith monomers is initiated by UV light, the channels can be photolithographically patterned. This allows polymer to be cast selectively. Using the mask, the polymerization is restricted to UV-exposed regions and monomers from the unexposed regions are flushed after the irradiation step. This approach is very valuable for the preparation of tailored microchip applications. The ability to photopattern also facilitate multidimensional separations by enabling multiple separate stationary phases in a single microchip.

First example of photoinitiated monolithic stationary phase for microchip-based monolithic CEC was developed and characterized by Ngola et al. [48]. Negatively charged monolith was based on butyl, hexyl and lauryl acrylate polymer. The zeta potential, charge and charge density were adjusted by changing the identity and concentration of the charged monomer. The polymers were able to support EOF as cast, thus did not require pressure-driven flow to flush the system. This also facilitated the possibility of the immediate use of prepared monolithic microchip column. Monolithic phase showed good performance for separation of three polycyclic aromatic hydrocarbons. Further optimization of casting process led into the system capable to separate 13 PAHs [49].

Negatively charged lauryl acrylate-based monoliths were used for the reverse phase electrochromatographic separation of bioactive peptides and amino acids in a glass-based microchip device [50,51]. The schematic of such a microchip device is shown in Fig. 9. The polymerization process was photoinitiated and monoliths were cast in situ in less than 10 min. As in previous work, solvent used to cast allowed EOF. Stationary phases prepared in this work were stable for period of several months and showed high separation efficiency with theoretical plate height up to 1.7 μm. Authors also developed a method for thermal decomposition of mono-

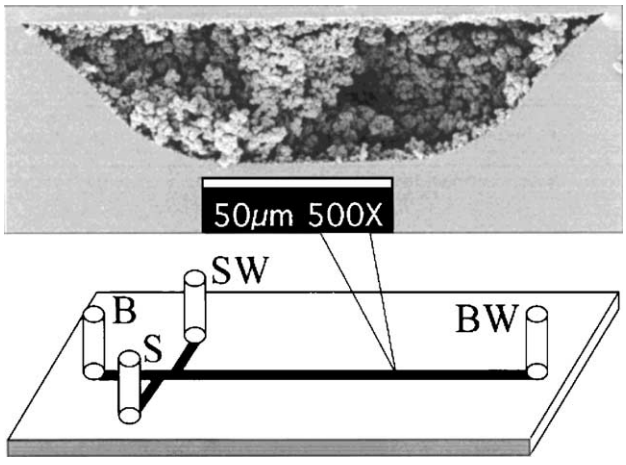

Fig. 9. Schematic of the polymer-based monolithic μCEC. B, S, BW and SW denote reservoirs containing buffer, sample, buffer waste and sample waste, respectively. The inset shows a scanning electron micrograph of a channel cross section filled with photoinitiated acrylate polymer monolith. The mean pore diameter is 1 μm. Reprinted from ref. [51] with permission.

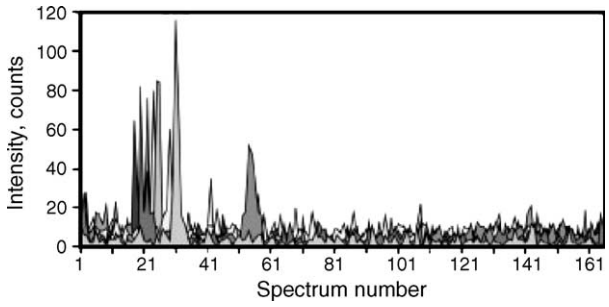

Fig. 10. Monolithic μCEC separation and MS detection of a protein digest. *Conditions:* bovine hemoglobin digest (0.8 mM); 6 cm separation channel; eluent, 15 mM CH_3COONH_4 (pH 4.6)/CH_3OH, 70:30 (v/v); field strength during m-μCEC run, 350 V/cm. Reprinted from ref. [52] with permission.

lithic polymer and its complete removal from microchip. The recovery of the chips considerably decreases the cost of the design prototyping.

Positively charged monolithic column was prepared for μCEC separation and mass-spectrometric detection of peptides [52]. The monolith was constructed from glycidyl methacrylate, methyl methacrylate and ethylene glycol dimethacrylate by photoinitiated polymerization. Consequently, surface of the monolith was rendered by ethylbutyl amine and baked overnight in the oven. In acidic mobile phase, amine groups generated positively charged surface and ethyl and butyl moieties enabled reverse phase separations. A positively charged monolithic stationary phase had improved separation performance for the separation of positively charged peptide mixtures in acidic eluents compared to negatively charged monoliths. A bovine hemoglobin digest was utilized to evaluate the performance of m-μCEC–MS configuration (as shown in Fig. 10) [52].

Morishima et al. used photopolymerized sol–gel (PSG) stationary phase [53]. PSG monolith was synthesized in the separation channel of a borosilicate glass chip via 5 min UV irradiation of a mixture of 3-methacryloxypropyltrimethoxysilane (MPTMS), hydrochloric acid (catalyst) and toluene (porogene). A sol–gel colloidal precursor of the PSG was formed in this solution through a series of hydrolysis and condensation reactions, described in detail in ref. [54]. PSG monolith supported electroosmotic flow without the need of pretreatment of the glass channel surface. Two neutral fluorescent dyes coumarin 314 and 510 were successfully separated in 225 s when detection occurred immediately after the 47 mm long PSG section. By moving the detection window along the separation channel (12 mm from the start of the PSG monolith), the analysis time was shortened to 80 s while analytes were baseline resolved.

It is also important to mention the work done by Frechet and co-workers on a preparation of photoinitiated monolithic stationary phases for conventional CEC [55,56], since their technology could be easily transferred into microchip format. Further information on conventional CEC monolithic stationary phases can be found in detailed review [57].

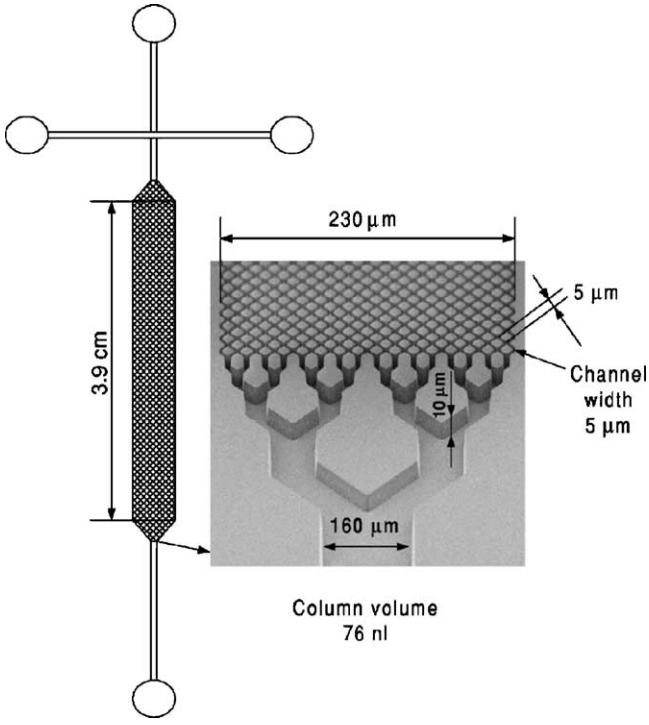

Fig. 11. Scheme of a typical COMOSS monolithic-μCEC separation column with detailed inlet section. Whole column was microfabricated using PDMS substrate. Reprinted from ref. [63] with permission.

2.3.2. *Monoliths prepared by microfabrication*

Regnier and co-workers introduced an alternative approach by which stationary phase support structures with dimensions of few micrometers (called "collocate monolith support structures"—COMOSS) were formed photolithographically inside the separation channel simultaneously with microchip manifold. This is a great example of the power of micromachining. The support structure arrays can be defined in size and position within 0.1 μm thus their distribution is extremely uniform (for example of such a column, see Fig. 11). Since COMOSS are an integral part of microfluidic device, they are secured from moving during the μCEC operations. Moreover, the channel dimensions are independent of any packing process and channel width can be varied independently of the size and shape of the support structures. The COMOSS microchannels are coated by stationary phase to facilitate μCEC separations [58–64]. The parameters of all COMOSS columns are summarized in Table 3. The initial work was performed with quartz structures [58–60]. Authors studied several options of support architecture (i.e. cylindrical and diamond shape), including the design of wall-effect compensating architecture, as shown in Fig. 12. Note that in the early work [58,59] authors used only one compound mixture (rhodamine 123) to evaluate the column efficiency and no effort was done to show the separation of two or more compounds. However, since the fabrication of quartz chips is expensive and work-consuming, prototyping of wide variety of COMOSS-based monolithic chips was carried out using polymeric PDMS substrate [61–64].

Table 3
Monolithic stationary phase microchip electrochromatography (m-μCEC)

Stationary phase/chip material	Initiation	Mobile phase	Bed dimensions (width[a] × depth × length)	Analyte	Time of analysis	Efficiency (H) (μm)	Reference
C_3 and SO_3^-/quartz	Chemical	Sodium phosphate (5 mM, pH 2.5), with 30% (for separation of alkylphenones) or 70% (for separation of antidepressants) (v/v) acetonitrile; sodium phosphate (5 mM, pH 7.4), with 15% (v/v) acetonitrile for separation of uracyl, phenol and benzyl alkohol model separation)	40 μm × 20 μm × 281 mm	Alkylphenones (acetophenone; propiophenone; butyrophenone; 2,6-dihydroxyacetophenone; 2,5-dihydroxypropiophenone, aniline) or antidepressants (nortriptyline, amitriptyline, methyl amitriptyline); uracyl, phenol and benzyl alcohol	20 s (for uracyl, phenol and benzyl alkohol); 9 min (for antidepressants); 18 min (for alkylphenones)	∼3	[46]
C_4, C_6, C_{12}/glass	Photo	Tris (5 mM, pH 8.5) with 80% (v/v) of acetonitrile	50 μm × 25 μm × 60 mm	PAHs (fluorene, chrysene, benz[*a*]pyrene)	23 s	∼5	[48]
C_{12}/glass	Photo	Tris (5 mM, pH 8.5) with 80% (v/v) of acetonitrile	50 μm × 25 μm × 70 mm	PAHs (naphthalene, acenaphthylene, acenaphthene, fluorene, phenanthrene, anthracene, fluoranthene, pyrene, benz[*a*]anthracene, chrysene, benz[*b*]fluoranthene, benzo[*k*]fluoranthene, benzo[*a*]pyrene	15 min	5	[49]
C_4, C_{12}/glass	Photo	Phosphate (12.5 mM, pH 7.0) with 35% (v/v) acetonitrile	50 μm × 25 μm × 80 mm	Bioactive peptides (papain inhibitor, α-casein, Ile–angiotensin III)	180 s	N/A	[50]
C_{12}/glass	Photo	Borate (25 mM, pH 8.2) with 30% (v/v) acetonitrile for separation of peptides; borate (20 mM) with 10% (v/v) acetonitrile for separation of amino acids	90–130 μm × 25–40 μm × 60 mm	Bioactive peptides (papain inhibitor, proctolin, opioid peptide, angiotensin III, Ile-angiotensin III, GGG) or amino acids (Arg, Ser, Gly, Phe, Trp)	45 s (pepties); 100 s (amino acids)	1.7	[51]

Sol–gel/glass	Photo	Ammonium acetate (12.5 mM, pH 6.5) with 60% (v/v) acetonitrile	90 μm × 35 μm × 47 mm	Coumarin dyes (314 and 510)	80 s	47	[53]
C_2 and C_4/glass	Photo/chemical	Ammonium acetate (15 mM, pH 4.6) with 30% (v/v) methanol	130 μm × 50 μm × 60 mm	Bovine hemoglobin tryptic digest	10 min	16	[52]
Phenyl/quartz	Chemical	Potasium phosphate (10 mM, pH 7.0)	150 μm × 10 μm × 45 mm (COMOSS diameters 5 μm × 5 μm × 10 μm; COMOSS spacing 1.5 μm)	Rhodamine 123 (only one compound mixture to test column performance)	130 s	1.3	[58]
C_{18}, phenyl/quartz	Chemical	Potasium phosphate (10 mM, pH 7.0)	150 μm × 9 μm × 45 mm (COMOSS diameters 5 μm × 5 μm × 9 μm; COMOSS spacing 1.5 μm)	Rhodamine 123 (only one compound mixture to test column performance)	130 s	1.3	[59]
C_{18}/quartz	Chemical	Potasium phosphate (10 mM, pH 9.0) with 25% (v/v) acetonitrile	150 μm × 10 μm × 45 mm (COMOSS diameters 5 μm × 5 μm × 10 μm; COMOSS spacing 1.5 μm)	Ovalbumin tryptic digests	600 s	N/A	[60]
C_8, C_{18}/PDMS	Chemical	Carbonate buffer (1 mM, pH 8.7) with 0.2% SDS	342 μm × 10 μm × 39 mm (COMOSS diameters 10 μm × 10 μm × 10 μm; COMOSS spacing 5 μm)	Rhodamine 110 and fluorescein; bovine serum albumine tryptic digest	200 s	2.5	[61]
Phenyl or C_4 or C_{18}/PDMS	Chemical	Carbonate buffer (1 mM, pH 9.0)	230 μm × 10 μm × 39 mm (COMOSS diameters 5 μm × 5 μm × 10 μm; COMOSS spacing 5 μm)	Short labeled peptides FITC–Gly–Phe–Glu–Lys (FITC)–OH, FITC–Gly–Phe–Glu–Lys–OH, FITC–Gly–Tyr–OH and FITC or bovine serum albumin digest	50 s short peptides; 300 s albumin digest	1.6	[63]
C_4/PDMS	Chemical	Carbonate buffer (1 mM, pH 9.0)	230 μm × 1.6–10 μm × 10–39 mm (COMOSS diameters from 5 μm × 5 μm × 1.6 μm to 11 μm × 11 μm × 10 μm; COMOSS spacing 2–4 μm)	Rhodamine 110 and fluorescein	35 s	1.6	[62]
C_4/PDMS	Chemical	1 mM phosphate buffer	230 μm × 10 μm × 39 mm (COMOSS diameters 5 μm × 5 μm × 10 μm; COMOSS spacing 3 μm)	Protein tryptic digest	150 s	N/A	[64]

[a] Channel width at half-height ($w_{1/2}$).

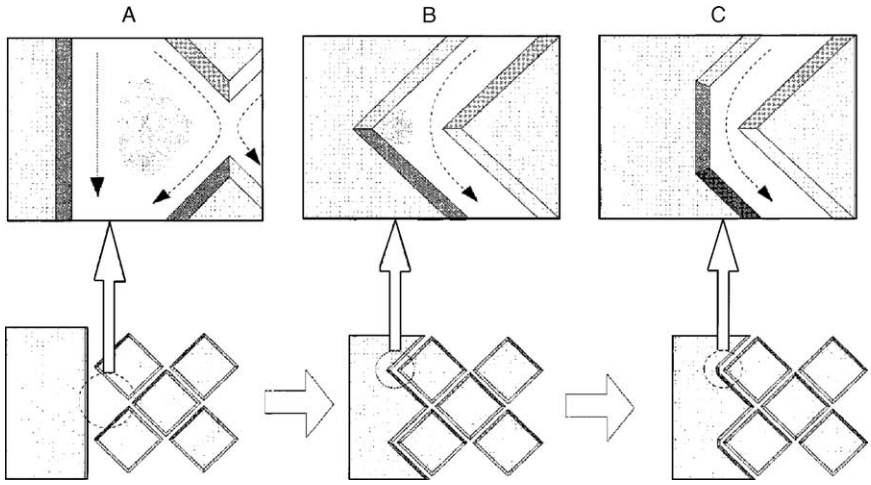

Fig. 12. Potential "wall effects" in micromachined columns of nominal 1.5-μm spacing width. (A) Large voids at the column–wall interface in a noncompensated architecture. The shaded area represents the volume of mobile phase that is poorly swept and has some stagnant character. It should also be noted that the distance to stationary-phase-bearing surfaces is greater at some points than the 2-μm diffusion distance required to control mobile-phase mass-transfer limitations. (B) Partially compensated architecture. The shaded area indicates that the volume of stagnant mobile phase has been substantially reduced. Diffusion distances to the stationary phase have also been reduced. (C) A fully compensated column–wall interface architecture. Note the elimination of stagnant mobile-phase pools. Reprinted from ref. [58] with permission.

PDMS material allowed fabrication of 20 COMOSS columns with different design and dimensions. Columns with different channel depth (1.6–10 μm) and COMOSS spacing (2–4 μm) were studied; the size of collocated columns (particles) was also varied, including hexagonal and diamond-like structures with their variations (5 μm × 5 μm to 11 μm × 11 μm). It was found that the column shape had an impact on bandspreading. The low aspect ratio structures were more efficient than their high aspect ratio (prolonged) equivalents. Diamond-like geometry was found to be the optimal shape for COMOSS-based separation systems. The highest efficiency of $H = 1.6$ μm was obtained with 10 μm deep channels and particles of 5.2 μm × 5.2 μm of diamond shape [62].

Since bare oxidized PDMS chips do not facilitate COMOSS–μCEC separations, the surface of PDMS device was coated by C_8 and C_{18} stationary phases. This stationary phase was capable to separate rhodamine and fluorescein and partly resolve peptides from BSA tryptic digest [61]. A problem with oxidized PDMS-based systems with C_8 or C_{18} moieties is low reproducibility and stability of EOF, since electroosmosis is based solely on dissociation of residual surface silanols. To overcome this limitation, Slentz et al. introduced several charged polymers on PDMS–COMOSS surface by cerrium (IV) catalyzed polymerization [63]. 2-Acrylamido-2-methylpropanesulfonic acid (AMPS), acrylic acid (AA), vinylsulfonic acid (VSA) and 4-styrenesulfonic acid (SSA) were tested as EOF promoters for the effective separation of peptide mixtures. While all promoters generated strong and stable electroosmotic flow, those with hydrophobic groups (phenyl and isobutyl of SSA and AMPS, respectively) also provided baseline separation of mixture of four short peptides. Furthermore, the AMPS-based polymer showed long-term stability and high efficiency ($H = 3.3$ μm). To improve efficiency and selectivity of AMPS-based column even more, AMPS–PDMS column was subsequently derivatized by methoxydimethyloctadecylsilane, additionally providing C_{18} moiety. Such stationary phase was successfully used for baseline and highly efficient ($H = 1.6$ μm) separation of short peptides and separation peptides of bovine serum albumin digest.

Truly comprehensive lab on chip format was demonstrated for proteomic analysis [64]. It consisted of on-chip tryptic digestion, copper(II) immobilized metal affinity chromatography selection of peptides containing histidin, and RP-COMOSS electrochromatography. Tripsin digestion and affinity chromatography was carried out in particle-based column with microfabricated frits, while m-μCEC separation was achieved on COMOSS column. All operations were driven by electroosmotic flow.

3. Conclusions and future prospects

Although a number of techniques for microchip-based electrochromatographic separations of charged and neutral compounds have been developed, the μCEC is still in a state of growth with a great future potential. The published papers showed that the reduced dimensions of microchip separation devices have the real advantage over conventional CEC. The contribution of the resistance to mass transfer decreases as the dimensions of the channel decrease as predicted by theory. This principle is greatly exploited in o-μCEC. Planar microchip format facilitate fully automated repetitive loading and removing of stationary phase in p-μCEC. Also, since EOF velocity is independent from particle size, it is possible to use stationary phase with small diameters down to 1.5 μm without having the large pressure drop, typical for LC. In

monolithic μCEC, photoinitiated polymerization allows to create stationary phase at the specific places of microfluidic network allowing tailored applications. The inherent way of microfabrication of microfluidic network by photolithography opens new avenues for simultaneous microfabrication of build-in monolithic columns.

Future development of novel stationary phases in o-μCEC can be foretold, very promising are, i.e. the nanoparticle-based materials. Intensive activity in improving stability of longer packed beds in p-μCEC can be foreseen in near future, since conventional silica-based phases are easily available and have well-defined and well-known properties. A widespread of lithographic fabrication of COMOSS monolithic columns can be expected in near future. As robust stationary phases for microchannel CEC will become commercially available, the μCEC methods will receive a wide acceptance in the future.

Acknowledgement

This work was supported by NATO Science Program.

References

[1] A. Manz, D.J. Harrison, E. Verpoorte, J.C. Fettinger, A. Paulus, H. Ludi, H.M. Widmer, J. Chromatogr. 593 (1992) 253–258.
[2] D. Figeys, D. Pinto, Anal. Chem. 71 (2000) 330A–335A.
[3] D.R. Reyes, D. Iossifidis, P.-A. Auroux, A. Manz, Anal. Chem. 74 (2002) 2623–2636.
[4] P.-A. Auroux, D.R. Reyes, D. Iossifidis, A. Manz, Anal. Chem. 74 (2002) 2637–2652.
[5] E. Verpoorte, Electrophoresis 23 (2002) 677–712.
[6] T. Vilkner, D. Janasek, A. Manz, Anal. Chem. 76 (2004) 3373–3386.
[7] D. Belder, M. Ludwig, Electrophoresis 24 (2003) 3595–3606.
[8] S. Eeltink, G.P. Rozing, W.T. Kok, Electrophoresis 24 (2003) 3935–3961.
[9] V. Dolnik, S. Liu, S. Jovanovich, Electrophoresis 21 (2000) 41–54.
[10] M.L. Chabinyc, D.T. Chiu, J.C. McDonald, A.D. Stroock, J.F. Christian, A.M. Karger, G.M. Whitesides, Anal. Chem. 73 (2001) 4491–4498.
[11] M. Pumera, J. Wang, F. Opekar, I. Jelínek, J. Feldman, H. Löwe, S. Hardt, Anal. Chem. 74 (2002) 1968–1971.
[12] C.T. Culbertson, S.C. Jacobson, J.M. Ramsey, Anal. Chem. 72 (2000) 5814–5819.
[13] M.J. Madou, Fundamentals of Microfabrication, CRC Press, Boca Raton, 2002.
[14] S.C. Jacobson, R. Hergenröder, L.B. Koutny, J.M. Ramsey, Anal. Chem. 66 (1994) 2369–2373.
[15] M.J.E. Golay, in: D.H. Desty (Ed.), Gas Chromatography, Butterworths, London, 1958, p. 36.
[16] J.W. Jörgenson, E.J. Guthrie, J. Chromartogr. 255 (1983) 335–338.
[17] S. Constantin, R. Freitag, D. Solignac, A. Sayah, M.A.M. Gijs, Sens. Actuators B 78 (2001) 267–272.
[18] S.A. Soper, S.M. Ford, S. Qi, R.L. McCarley, K. Kelly, M.C. Murphy, Anal. Chem. 72 (2000) 642A–651A.
[19] M. Galloway, W. Stryjewski, A. Henry, S.M. Ford, S. Llopis, R.L. McCarley, S.A. Soper, Anal. Chem. 74 (2002) 2407–2415.
[20] M. Galloway, S.A. Soper, Electrophoresis 23 (2002) 3760–3768.
[21] A.C. Henry, T.J. Tutt, M. Galloway, Y.Y. Davidson, C.S. McWhorter, S.A. Soper, R.L. McCarley, Anal. Chem. 72 (2000) 5331–5337.
[22] S.A. Soper, A.C. Henry, B. Vaidya, M. Galloway, M. Wabuyele, R.L. McCarley, Anal. Chim. Acta 470 (2002) 87–99.
[23] X. Cahours, P. Morin, M. Dreux, J. Chromatogr. A 845 (1999) 203–216.
[24] A.L. Crego, J. Martinez, M.L. Marina, J. Chromatogr. A 869 (2000) 329–337.
[25] J.P. Kutter, S.C. Jacobson, J.M. Ramsey, Anal. Chem. 69 (1997) 5165–5171.
[26] M.J. Sepaniak, D.F. Swaile, A.C. Powell, J. Chromatogr. 480 (1989) 185–196.
[27] J.P. Kutter, S.C. Jacobson, N. Matsubara, J.M. Ramsey, Anal. Chem. 70 (1998) 3291–3297.
[28] B.S. Broyles, S.C. Jacobson, J.M. Ramsey, Anal. Chem. 75 (2003) 2761–2767.
[29] N. Gottschlich, S.C. Jacobson, C.T. Culbertson, J.M. Ramsey, Anal. Chem. 73 (2001) 2669–2674.
[30] R.D. Rocklin, R.S. Ramsey, J.M. Ramsey, Anal. Chem. 72 (2000) 5244–5249.
[31] J.D. Ramsey, S.C. Jacobson, C.T. Culbertson, J.M. Ramsey, Anal. Chem. 75 (2003) 3758–3764.
[32] M. Pumera, J. Wang, E. Grushka, R. Polsky, Anal. Chem. 73 (2001) 5625–5628.
[33] Y.-W. Lin, M.-J. Huang, H.-T. Chang, J. Chromatogr. A 1014 (2003) 47–55.
[34] B. Neiman, E. Grushka, O. Lev, Anal. Chem. 73 (2001) 5220–5227.
[35] G.M. Gross, D.A. Nelson, J.W. Grate, R.E. Synovec, Anal. Chem. 75 (2003) 4558–4564.
[36] W. Xu, K. Uchiyama, T. Shimosaka, T. Hobo, J. Chromatogr. A 907 (2001) 279–289.
[37] W. Xu, K. Uchiyama, T. Hobo, Chromatography 23 (2002) 131–138.
[38] J. Wang, A. Muck Jr., M.P. Chatrathi, G. Chen, N. Mittal, S.D. Spillman, S. Obeidat, Lab. Chip 5 (2005), in press.
[39] R.D. Oleschuk, L.L. Schultz-Lockyear, Y. Ning, D.J. Harrison, Anal. Chem. 72 (2000) 585–590.
[40] A.B. Jereme, R.D. Oleschuk, F. Ouchen, G. Fajuyigbe, D.J. Harrison, Electrophoresis 23 (2002) 3537–3544.
[41] A.B. Jereme, R.D. Oleschuk, D.J. Harrison, Electrophoresis 24 (2003) 3018–3025.
[42] L. Ceriotti, N.F. Rooij, E. Verpoorte, Anal. Chem. 74 (2002) 639–647.
[43] G.A. Lord, D.B. Gordon, P. Myers, B.W. King, J. Chromatogr. A 768 (1997) 9–16.
[44] R. Jindal, S.M. Cramer, J. Chromatogr. A 1044 (2004) 277–285.
[45] K.W. Ro, W.-J. Chang, H. Kim, J.M. Koo, J.H. Hahn, Electrophoresis 24 (2003) 3253–3259.
[46] C. Ericson, J. Holm, T. Ericson, S. Hjertén, Anal. Chem. 72 (2000) 81–87.
[47] J.H. Knox, J.F. Parcher, Anal. Chem. 41 (1969) 1599–1606.
[48] S.M. Ngola, Y. Fintschenko, W.-Y. Choi, T.J. Shepodd, Anal. Chem. 73 (2001) 849–856.
[49] Y. Fintschenko, W.-Y. Choi, S.M. Ngola, T.J. Shepodd, Fresenius J. Anal. Chem. 371 (2001) 174–181.
[50] R. Shediac, S.M. Ngola, D.J. Throckmorton, D.S. Anex, T.J. Shepodd, A.K. Singh, J. Chromatogr. A 925 (2001) 251–263.
[51] D.J. Throckmorton, T.J. Shepodd, A.K. Singh, Anal. Chem. 74 (2002) 784–789.
[52] I.M. Lazar, L. Li, Y. Yang, B.L. Karger, Electrophoresis 24 (2003) 3655–3662.
[53] K. Morishima, B.D. Bennett, M.T. Dulay, J.P. Quirino, R.N. Zare, J. Sep. Sci. 25 (2002) 1226–1230.
[54] M.T. Dulay, J.P. Quirino, B.D. Bennett, M. Kato, R.N. Zare, Anal. Chem. 73 (2001) 3921–3926.

[55] C. Yu, F. Svec, J.M.J. Frechet, Electrophoresis 21 (2000) 120–127.
[56] C. Yu, M.C. Xu, F. Svec, J.M.J. Frechet, J. Polym. Sci., Part A: Polym. Chem. 40 (2002) 755–769.
[57] E.F. Hilder, F. Svec, J.M.J. Frechet, Electrophoresis 23 (2002) 3934.
[58] B. He, N. Tait, F. Regnier, Anal. Chem. 70 (1998) 3790–3797.
[59] B. He, F. Regnier, J. Pharm. Biomed. Anal. 17 (1998) 925–932.
[60] B. He, J. Ji, F. Regnier, J. Chromatogr. A 853 (1999) 257–262.
[61] B.E. Slentz, N.A. Penner, E. Lugowska, F. Regnier, Electrophoresis 22 (2001) 3736–3743.
[62] B.E. Slentz, N.A. Penner, F. Regnier, J. Sep. Sci. 25 (2002) 1011–1018.
[63] B.E. Slentz, N.A. Penner, F. Regnier, J. Chromatogr. A 948 (2002) 225–233.
[64] B.E. Slentz, N.A. Penner, F. Regnier, J. Chromatogr. A 984 (2003) 97–107.